

To Move or Not to Move: Constraint-based Planning Enables Zero-Shot Generalization for Interactive Navigation

Apoorva Vashisth
Purdue University
USA

vashista@purdue.edu

Manav Kulshrestha
Purdue University
USA

mkulshre@purdue.edu

Pranav Bakshi
IIT Kharagpur
India

pb@gmail.com

Damon Conover
DEVCOM Army Research Lab
USA

damon.m.conover.civ@army.mil

Guillaume Sartoretti*
National University of Singapore
Singapore

guillaume.sartoretti@nus.edu.sg

Aniket Bera*
Purdue University
USA

ab@cs.purdue.edu



Figure 1. Demonstration of our approach deployed on the Boston Dynamics Spot robot. The left image shows the region of the environment that is the robot’s operating area for the current task, initially unknown. The robot first observes the scene and determines presence of task-relevant objects (Bottle and Desk in this case). Based on the observations and the current task progress, the robot determines the best course of action (“Bring RedBottle to Desk2”). Here, based on the current episode progress (4 out of total 20 tasks completed) and cost-benefit analysis (moving potential clutter vs directly completing the task), it decides to first optimize the environment by moving clutter (the paper towel roll) and storing it at a carefully chosen spot out of the way (the black box). The robot is then able to place the red bottle on the desk.

Abstract

Visual navigation typically assumes the existence of at least one obstacle-free path between start and goal, which must be discovered/planned by the robot. However, in real-world scenarios, such as home environments and warehouses, clutter can block all routes. Targeted at such cases, we introduce the **Lifelong Interactive Navigation** problem, where a mobile robot with manipulation abilities can move clutter to forge its own path to complete sequential object-placement tasks – each involving placing an given object (eg. Alarm clock, Pillow) onto a target object (eg. Dining table, Desk, Bed). To address this lifelong setting – where effects of environment changes accumulate and have long-term effects – we propose an LLM-driven, constraint-based planning framework with active perception. Our framework allows the LLM to reason over a structured scene graph of discovered objects and obstacles, deciding which object to

move, where to place it, and where to look next to discover task-relevant information. This coupling of reasoning and active perception allows the agent to explore the regions expected to contribute to task completion rather than exhaustively mapping the environment. A standard motion planner then executes the corresponding navigate–pick–place, or detour sequence, ensuring reliable low-level control. Evaluated in physics-enabled ProCThor-10k simulator, our approach outperforms non-learning and learning-based baselines. We further demonstrate our approach qualitatively on real-world hardware¹.

1. Introduction

Visual navigation has achieved remarkable progress in recent years via advances in embodied simulation [9], generative models [1, 36], and deep learning [15, 22]. However, most navigation systems assume that there exists at

*These authors jointly supervised this work.

¹We will release our code and dataset upon acceptance.

least one obstacle-free path between start and goal locations. This assumption holds in idealized cases, but may not hold in real-world scenarios such as homes and warehouses, where clutter, furniture, and everyday objects can obstruct all routes to the goal. In such settings, navigation alone is insufficient and robots must take agency over their environment rather than merely reacting to it. With modern mobile manipulators increasingly equipped with arms, grippers, and perception modules, they are no longer just sensors on wheels but embodied agents capable of reshaping their surroundings to achieve their goals. In these cases, an agent must do more than navigate: it must reconfigure its environment to make progress.

Existing visual navigation frameworks are typically brittle under such conditions. Reactive planners [5, 13] often detour around occlusions, while learned policies [16, 28] fail to generalize to new environments. Interactive navigation methods [30, 35] have begun to address this gap, but are commonly defined for a single task at a time, often pre-arranged such that interaction is the only solution, and assume full observability of the environment. In contrast, real robots face sequential streams of tasks in the same dynamic space, where each decision (to move or not to move an object) carries lasting consequences for future goals.

In this work, we introduce the *Lifelong Interactive Navigation* problem, where a mobile manipulator receives a sequence of navigation-and-manipulation objectives in an unknown environment, each requiring placement of a given object (eg. Basketball, Alarm Clock) onto a target object (eg. Bed, Arm Chair). This requires the agent to continuously reason about where to explore, which obstacles to remove, which to bypass, and future impact of these choices. Crucially, planning and perception are tightly coupled: the agent not only plans about how to act but also where to look next to reveal task-relevant objects. While moving obstacles could open up previously unavailable routes at a nontrivial manipulation cost, detouring may save effort while restricting future mobility. Success thus depends not only on short-term feasibility but also on long-horizon, perception-aware reasoning over the evolving environment.

Large language models can reason over structured and semantic inputs, with their strengths demonstrated in abstract reasoning rather than in producing fine-grained control sequences. Our key insight is to invert the typical interface between language models and embodied agents: we recast the LLM’s role from action sequence generator to a constraint reasoner, operating over the structure of the environment. Our structured scene graph, continuously updated with perceptual feedback to include new objects, rooms, and spatial relationships, serves as the LLM’s input representation. The frozen LLM then treats each blocking object as a decision point and determines whether to intervene – i.e., whether moving the obstacle will substantially expand

navigable space given the movement cost – or if it can be safely detoured around without significant impact on long-term performance. By re-framing planning as constraint resolution problem, we transform long-horizon reasoning from chaining low-level steps into making a small number of strategic, semantically grounded decisions. This shift enables zero-shot LLM planning, without task-specific fine-tuning, while tightly coupling perception and reasoning.

Building on this constraint-driven formulation, we evaluate our framework in the ProcTHOR-10k [4] simulator, which offers visually rich, physics-enabled conditions. Our task suite is augmented with cluttered object configurations across environments consisting of up to ten rooms. Each episode involves sequential tasks (e.g., bringing object X to receptacle Y), where the robot receives each new task only after completing the previous one. The robot has no prior knowledge of future tasks – if it fails to complete a task, the episode terminates immediately, and it does not receive any subsequent tasks. Hence, later in the episode, success depends not only on efficient exploration but also on strategic environment modification, as earlier decisions (such as whether to move or detour around obstacles) can significantly influence accessibility to regions containing the target objects, and later progress. By evaluating our system in this online task sequence framework, we test the real-world applicability of our approach, which must adapt in real time without knowledge of future goals. The key contributions of our work include:

- Lifelong Interactive Navigation: Extending prior interactive navigation problem to long-horizon, sequential tasks in unknown environments.
- Constraint-based planning framework: Shifting the decision space from low-level actions to high-level environmental constraints, enabling zero-shot long-horizon reasoning by large language models.
- Our method achieves the highest Long-term Efficiency Score (LES), improving over the strongest non-learned baseline by 20 – 50%, and outperforming prior interactive navigation methods by 3–6× in larger environments.

2. Related Work

Embodied and Visual Navigation. Visual navigation has been extensively studied as mapping observations to actions under the implicit assumption of existence of at least one obstacle-free path between start and goal. Early works and benchmarks such as Cognitive Mapping and Planning [7], Target-driven Navigation [40], AI2-THOR [9], Gibson [33], Habitat [19, 26], and ProcTHOR [4] have driven progress toward robust policies in visually rich, partially observed environments. Subsequent methods improve exploration and representation via generative models, memory, and structured scene reasoning [1, 10, 12, 21, 36–38], and tackle image-goal, language-driven, and multi-object

navigation [6, 14, 25, 29, 34, 39]. However, these methods treat the environment as static and ultimately traversable: agents search more efficiently, predict unseen regions, exploit priors over layouts, or decompose the task, but if all geometric routes to the goal are blocked by clutter, they can only attempt detours or fail. In contrast, our problem setting explicitly targets cluttered, potentially non-traversable environments, enabling a mobile manipulator to reason about “whether, where and which” obstacles to move, reconfiguring the environment to restore or improve connectivity for long-horizon task sequences.

Interactive Navigation & Navigation Among Movable Obstacles (NAMO). A parallel line of work studies Navigation Among Movable Obstacles, where an agent may relocate objects to reach a blocked goal. Classical NAMO and rearrangement planners search over joint spaces of robot motion and obstacle configurations [2, 3, 11, 17, 18, 23, 24, 32], but assume full knowledge of geometry and dynamics, small number of obstacles, and short horizons, while optimizing reaching a single goal rather than reasoning about persistent environmental changes or future tasks. Interactive navigation approaches bring these ideas into embodied setting: Interactive Gibson [33] provides benchmarks for interaction in clutter; InterNav [35] and CaMP [30] learn how to move blocking objects based on visual input. Interactive-FAR [8], IN-Sight [20], ADIN [31], SPIN [27], and related systems for legged manipulators or human-in-the-loop assistance explore fast heuristics, affordances, or uncertainty-aware querying for interactive routing.

However, these systems remain fundamentally reactive: their objective is to locally circumvent or temporarily push aside visible obstacles rather than reason about how environment modifications influence future accessibility. They are typically designed per-episode and per-task, often in cluttered scenes constructed to necessitate one-off interactions. Once the sole task is achieved, the episode ends and the environment resets, eliminating any need to consider the long-term consequences of manipulation. As a result, these methods focus on short-horizon obstacle removal rather than persistent environment restructuring. In contrast, our Lifelong Interactive Navigation framework operates in a sequential, no-reset setting where each decision carries lasting impact. The agent must determine not only “which” obstacles to move but also “where” to place them and “when” to refrain from interaction, reasoning over both spatial constraints and perceptual uncertainty to maximize long-term connectivity and task efficiency in a single evolving environment.

3. Our Approach

Overview. We target the Lifelong Interactive Navigation setting introduced in Sec. 1, where a mobile manipulator

receives a sequence of navigation-and-manipulation tasks in an initially unknown, cluttered environment. The central challenge is that not all tasks are reachable by pure navigation: some obstacles must be moved, some rooms must be explored, and each intervention can affect future tasks. To handle this, we decouple strategic long-horizon choices from tactical low-level control.

At time t , the agent maintains a partial environment state $\mathcal{E}_t = (\mathcal{O}_t, \mathcal{R}_t)$, where \mathcal{O}_t is the set of discovered objects/rooms and \mathcal{R}_t encodes their blocking and reachability relations. Our large language model (LLM) operates on a structured textual serialization of \mathcal{E}_t and reasons about how to resolve the current environmental constraints – deciding, for example, which obstacle to relocate, where to place it, or which room to investigate next. These high-level constraint resolutions are then converted by a low-level planner into concrete navigation and manipulation actions. Hence, we recast the LLM as a constraint reasoner over the environment: it determines “what to change in the world” rather than “how to move the robot step by step”.

Perception and structured scene construction. In this work, we assume that the general floor plan is known, but that room contents are unknown at first. We define a grid-graph $G = (N, E)$ that denotes the currently traversable region of the world. Here, nodes N correspond to the cells that the robot can occupy and edges E connect adjacent free cells, forming the basis for all path and connectivity computations. The environment is discovered incrementally through obtained RGB-D observations. After each view, the perception module detects visible objects and free space, and updates the grid-graph G with new traversable nodes, and a structured scene representation that also maintains the set of known yet unexplored rooms. Although the total number of rooms and their topological adjacencies are known from the underlying floorplan, the contents of each room and the traversability of the connecting passages must be inferred through exploration.

We represent the world state at time t as a directed graph $\mathcal{E}_t = (\mathcal{O}_t, \mathcal{R}_t)$, where nodes correspond to discovered objects or rooms, and edges encode blocking relations between them (e.g., an object obstructs the shortest path to another). Formally, for $o_i, o_j \in \mathcal{O}_t$,

$$C_{ij} = \begin{cases} 1, & \text{if } o_i \text{ blocks the shortest path to } o_j, \\ 0, & \text{otherwise.} \end{cases} \quad (1)$$

We utilize the grid graph G to describe the impact of an obstacle object on the navigability of the region. Let $n(o_i) \in N$ denote the node occupied by o_i . We compute

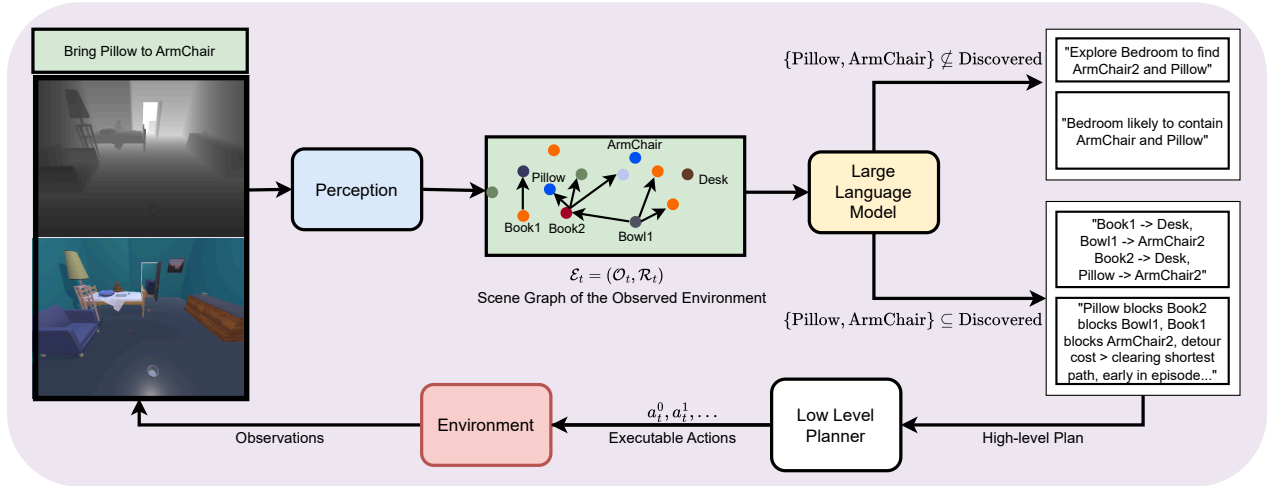


Figure 2. Overview of our constraint-based planning framework for interactive navigation. At each timestep, our agent receives observations from the environment, which are utilized by our perception module to update the scene graph. Our scene graph contains the observed objects of the environment as nodes and the blocking relation among them as edges. Each node has its own attributes, which provide additional navigability and manipulability context to the LLM. The LLM then decides whether to explore the environment further to collect additional information or to attempt to complete the given task based on the scene graph content and the environment constraints.

the (normalized) betweenness centrality of $n(o_i)$:

$$\text{bc}(n(o_i)) = \frac{1}{Z} \sum_{\substack{s \neq t \in N \\ s \neq n(o_i) \neq t}} \frac{|\sigma_{st}(n(o_i))|}{|\sigma_{st}|},$$

where $|\sigma_{st}|$ is the cardinality of the set of shortest paths σ_{st} between any node s and any node t where $s \neq t$, $|\sigma_{st}(n(o_i))|$ is the cardinality of the subset of the shortest paths that pass through $n(o_i)$, $\sigma_{st}(n(o_i))$, and Z is a normalization constant. This measures how many shortest paths depend on the node occupied by o_i , and thus how many paths would potentially become available if o_i were removed.

In our representation \mathcal{E}_t , each object node $o_i \in \mathcal{O}_t$ is augmented with attributes that capture both geometric and topological context for decision-making: (i) the cost of traversing the shortest path to the object, if it exists; (ii) the set of discovered objects that block this path, represented via $C_{ij} = 1$; (iii) the betweenness centrality $\text{bc}(n(o_i))$ of the grid cell occupied by the object in the grid graph $G = (N, E)$, measuring its influence on global connectivity; (iv) the cost of an alternative path that avoids all current blockers, if it exists. All path computations are performed on G , where only nodes and edges corresponding to currently observed free space are treated as traversable; unknown regions are never assumed passable until they are discovered. Unseen rooms are maintained as frontier nodes, serving as exploration candidates. After each executed action, \mathcal{E}_t is updated to incorporate newly discovered objects, newly navigable rooms, revised exploration status,

and obstacles that have been successfully removed.

LLM as a constraint-based planner. Given this text description of the scene graph, we use a frozen LLM to select the next high-level step. Intuitively, every blocking object is a decision point: should this object be relocated now, and if so, where, or can it be bypassed without significantly harming long-term performance? We formalize this as a cost-benefit selection over blocking objects.

For a candidate obstacle o_i , we define a removal cost that accounts for both the effort of manipulating the object and the effort of relocating it to a valid drop zone. To ensure they can be appropriately compared, both navigation and manipulation costs are estimated in terms of time:

$$\text{cost}(o_i, r_t, z_j) = d(r_t, o_i) + 2 \times e(o_i) + d(o_i, z_j),$$

where $d : N \times N \rightarrow \mathbb{R}^+$ describes the time taken to traverse the geodesic distance between two nodes. Hence, $d(r_t, o_i)$ is the cost of navigating from the robot's current position to the obstacle, $e(o_i)$ summarizes the manipulation effort for object o_i (time required to pick and place an object due to its physical attributes such as size and weight), and $d(o_i, z_j)$ is the cost of navigating the path from the obstacle's position to a feasible drop zone z_j . The values of $d(r_t, o_i)$ and $d(o_i, z_j)$ are estimated from the paths on the grid graph G . In our experiments, we use a static manipulation cost $e(o_i) = 5.00$ (seconds) (counted twice for pick-and-place actions). This setting reflects our empirical observation that a pick/place cycle – including approach, alignment, grasp execution, verification, and safety pauses – dominates base

travel time, and therefore the cost function should generally favor clearing tasks via short navigation movements over initiating unnecessary manipulations. The LLM reasons jointly over candidate pairs (o_i, z_j) , evaluating both the effort required to clear the object and the suitability of each drop zone (whether it is accessible, obstacles on the path, their attributes and their valid drop zones, etc.). We also present an ablation that varies the value of e to measure the sensitivity of our approach to this hyperparameter.

Conceptually, the planner is approximating the rule

$$o^*, z^* = \arg \min_{o_i \in \mathcal{O}_t, z_j \in \mathcal{Z}_t} (\text{cost}(o_i, r_t, z_j) - \text{bc}(n(o_i))), \quad (2)$$

and issues a Pick-and-Place action sequence for o^* when this trade-off is favorable. This formulation lets the LLM reason not only about which obstacle to move, but also where to place it, balancing manipulation cost, travel distance, and long-term navigability.

When no obstacle offers a sufficient gain, the planner first queries the current grid graph G to determine whether an alternate, collision-free path to the goal exists. If such a detour exists, the agent proceeds with a standard navigation sequence using the low-level planner, completing the task without manipulating any obstacles. If a detour does not exist, the planner attempts to move the minimum number of obstacles that would restore connectivity to achieve the task. If the goal objects have not been discovered, the planner initiates a task-directed. In this stage, the agent reasons over the set of known but unexplored (or partially explored) rooms and selects the next room to visit based on its semantic relevance to the current task. Specifically, given a task such as “bring vase to dining table”, the planner prioritizes rooms whose semantic types make them more likely to contain the missing entities (e.g., Living Room or Kitchen over Bathroom or Bedroom). Once the relevant objects have been discovered, the planner evaluates the connectivity between them. The planner identifies which obstacles block the paths and using the obstacle attribute, their drop zone attributes, manipulation costs, and number of remaining tasks, decides which obstacle to move and where.

While Eq. (2) defines a quantitative heuristic that balances manipulation cost with connectivity gain, it alone cannot capture the higher-order relational and semantic dependencies present in the environment. For example, deciding whether to move an obstacle depends on several factors such as remaining future tasks, long-term cost of detouring around the obstacle (if not moved), immediate cost of moving, and contextual constraints such as available drop zones and unexplored regions. Hence, in our framework, the LLM operates as a constraint reasoner, combining these quantitative estimates with commonsense and task-level reasoning to generate interpretable, semantically grounded plans that generalize beyond the scope of a

fixed heuristic.

Low-level planning and closed-loop execution. The execution of the LLM’s output plan is delegated to a standard motion stack that outputs a sequence of executable actions $[a_t^0, a_t^1, a_t^2, \dots]$. For navigation, we run a Dijkstra-based planner over the currently discovered and reachable subgraph to obtain collision-free paths to the target objects, obstacle objects, rooms, or drop zones. For manipulation, we treat pick-place as a reliable primitive provided by the underlying robot control stack, and assume that designated objects have sufficient free space for placement. This separation of concerns lets the LLM focus on long-horizon, semantically meaningful choices about which constraints to resolve (which object to move, where to relocate it, and when to explore), while the low-level planner ensures reliable navigation and manipulation control in cluttered, physics-enabled environments under our assumptions.

4. Experiments

4.1. Setup

Dataset. We first constructed a new dataset of cluttered indoor floors by instantiating ProcTHOR-10k simulator with procedurally generated clutter. We generate 10k episodes with 20 tasks each, following the Lifelong Interactive Navigation setup described in Sec. 1. For our test set, we randomly draw 100 environments equally distributed among the number of rooms 1 – 10. Following previous works [30], we group the environments by floorplan complexity and report the results in three categories: 1 – 3, 4 – 6, and 7 – 10. To generate realistic clutter in the environment, we occlude a percentage of traversable nodes (based on floorplan area) in the grid graph $G = (N, E)$ of an environment without obstacles, where the probability of a node $n \in N$ being selected for occlusion is proportional to its betweenness centrality $\text{bc}(n)$. This biases obstacle placement toward structurally critical regions such as hallways, bottlenecks, and intersections, without deterministically blocking all high-centrality nodes. Please refer to Appendix A for dataset visualization.

Evaluation Metrics. Our framework jointly optimizes three complementary objectives: (i) the success rate $\text{SR} = \frac{1}{N_{\text{episodes}}} \sum_{k=1}^{N_{\text{episodes}}} \frac{N_{\text{success}}^{(k)}}{N_{\text{goals}}^{(k)}}$, reflecting the agent’s ability to complete assigned tasks (where $N_{\text{success}}^{(k)}$ and $N_{\text{goals}}^{(k)}$ denote the number of successfully completed and total assigned goals in episode k , respectively); (ii) the time efficiency, measured by the number of timesteps required to finish each episode $\text{TS} = \frac{1}{N_{\text{episodes}}} \sum_{k=1}^{N_{\text{episodes}}} T_k$, (where T_k is the total number of timesteps in episode k); and (iii) the long-term environmental efficiency for navigation, which quantifies

Methods	1 – 3 rooms				4 – 6 rooms				7 – 10 rooms			
	SR↑	PoC↓	TS↓	LES↑	SR↑	PoC↓	TS↓	LES↑	SR↑	PoC↓	TS↓	LES↑
InterNav	16.67	1.96	842.00	0.0764	6.00	2.13	4700.70	0.0037	3.00	3.34	6089.91	0.0024
Always Detour	90.45	1.96	665.64	0.3788	83.18	2.15	1115.27	0.1644	<u>64.09</u>	3.43	1381.61	0.0661
Always Interact	100.00	<u>1.14</u>	1108.88	<u>0.4082</u>	100.0	<u>1.13</u>	2416.67	0.1707	100.00	1.36	3974.88	<u>0.0943</u>
Clean + S/P	100.00	1.00	1200.48	0.4297	100.00	1.00	2622.94	<u>0.1714</u>	100.00	1.00	5169.58	0.0841
Ours (unk)	88.94	1.48	1339.36	0.2753	81.67	1.81	3211.20	0.0598	62.27	2.79	4497.80	0.0344
Ours (known)	<u>94.55</u>	1.50	<u>1044.55</u>	0.3322	<u>97.73</u>	1.25	<u>1911.97</u>	0.1945	100.00	<u>1.23</u>	<u>2435.48</u>	0.1574

Table 1. Comparison of our approach with baselines across different floorplans. \uparrow indicates higher value is better for the metric, \downarrow indicates lower value is better for the considered metric. Bold indicates the best performance of the metric, while underline indicates second-best performance. Bold and underline is the best performance for the primary evaluation metric LES.

how the agent’s actions improve or degrade future navigability of the environment. As explained in Appendix B, we describe the last term using the ratio of the cumulative shortest-path lengths in the current cluttered environment to those in an obstacle-free configuration, termed as Price of Clutter - PoC = $\frac{\sum_{s,t \in V} d_{\text{obs}}(s,t)}{\sum_{s,t \in V} d_{\text{free}}(s,t)}$, where $d_{\text{obs}}(s,t)$ is the shortest-path distance between nodes s and t in the cluttered environment, and $d_{\text{free}}(s,t)$ is the corresponding distance in the obstacle-free floorplan.

While SR captures immediate task performance and TS measures execution speed, long-term optimization emphasizes maintaining a structured, uncluttered environment that facilitates subsequent tasks. To consolidate these competing objectives into a single measure, we introduce the globally normalized composite metric termed Long-term Efficiency Score (LES) which explicitly models the trade-off between short-term success (SR), temporal efficiency (TS), and sustainable environment restructuring (PoC):

$$\text{LES} = \frac{\text{SR} / \max(\text{SR})}{(\text{TS} / \min(\text{TS})) \times (\text{PoC} / \min(\text{PoC}))}. \quad (3)$$

A high LES indicates that a policy not only succeeds at the current task efficiently but also preserves or enhances the environment for future interactions. In this way, LES provides a holistic evaluation of an agent’s balance between immediate task completion, execution speed, and long-term environmental foresight. A high SR increases LES, while large TS or PoC reduce it, preventing any method from appearing artificially superior by favoring either short-term speed at the expense of completeness or exhaustive search at the expense of efficiency. We describe our metric LES in more detail in Appendix C.

4.2. Baseline Comparison

We compare our method against three heuristic baselines and one learning-based method, using identical goal sequences and obstacle placements. Since the four baselines assume ground-truth knowledge of the environment, we expose this information to one of our variants and thus report

metrics for two versions of our approach - Ours(unk), which has no a priori knowledge of the world and must explore the environment, and Ours (known), which has ground-truth knowledge of the world. Our baselines are -

- **InterNav (learning-based)** [35]: A policy trained end-to-end for interactive navigation.
- **Always Detour**: Never interacts with an obstacle and attempts to complete tasks using pure navigation.
- **Always Interact**: On encountering a blocking object along the shortest path to the goal, move the obstacle to the nearest valid drop zone.
- **Clean + S/P**: First removes all obstacles in the environment by relocating them to their nearest drop zones, then completes all tasks along (now available) shortest paths.

Tab. 1 summarizes the performance of the considered approaches. We report SR, TS, PoC, and LES across all floorplans. Across all rooms, ‘InterNav’ [35] performs worst as it has been designed for single-episode, short-horizon, local obstacle-clearing in small, cluttered rooms. When deployed in our multi-room, long-horizon environment with sequential manipulation tasks where success in future tasks is heavily dependant on past actions, it breaks down. In small layouts (1 – 3 rooms), the exhaustive strategies ‘Always Interact’ and ‘Clean + S/P’ obtain slightly higher LES than ours: with few rooms and short horizons, aggressive cleanup is not heavily penalized. However, as complexity increases (4 – 6 and 7 – 10 rooms), our method consistently achieves the highest LES, while the baselines deteriorate. ‘Always Interact’ and ‘Clean + S/P’ maintain high SR and low PoC, but suffer drastic growth in TS, resulting in low efficiency. Always Detour attains short TS but suffers for never resolving constraints with poor PoC and degraded SR. In contrast, our approach maintains strong SR with substantially lower TS than exhaustive cleanup and markedly better PoC than non-interactive detouring, indicating selective manipulation of structurally important obstacles. The gap between our two variants (known/unknown) reflects the intrinsic penalty of partial observability, where the agent must actively explore to infer the environment’s structure, incurring additional time costs and occasionally making suboptimal

Manipulation Effort	1 – 3 rooms				4 – 6 rooms				7 – 10 rooms			
	SR↑	PoC↓	IE	PL (m)↓	SR↑	PoC↓	IE	PL (m)↓	SR↑	PoC↓	IE	PL (m)↓
$e = 1$	<u>92.58</u>	1.44	42.21	302.73	83.79	1.46	41.09	646.35	<u>65.45</u>	2.65	36.09	999.48
$e = 5$	85.30	<u>1.48</u>	36.31	295.04	79.55	1.81	38.48	825.78	69.09	<u>2.79</u>	32.09	1057.96
$e = 10$	92.42	1.53	23.27	301.07	80.45	<u>1.62</u>	39.76	809.92	60.61	2.94	25.48	1211.33
$e = 15$	91.21	1.59	15.33	<u>287.38</u>	<u>80.91</u>	1.87	21.88	822.90	63.39	3.00	20.89	<u>1037.37</u>
$e = 20$	92.88	1.62	9.58	259.63	78.48	1.90	21.36	<u>715.82</u>	60.30	2.95	18.58	1078.59

Table 2. Effect of varying manipulation effort e on the behavior of our constraint-based LLM planner. ↑ indicates higher value is better, ↓ indicates lower value is better. Bold indicates the best performance of the metric while underline indicates second-best performance.

History Length	1 – 3 rooms				4 – 6 rooms				7 – 10 rooms			
	SR↑	PoC↓	TS↓	LES↑	SR↑	PoC↓	TS↓	LES↑	SR↑	PoC↓	TS↓	LES↑
$h = 1$	89.85	1.44	1793.97	0.3634	78.94	<u>1.67</u>	3516.03	0.0929	55.00	2.71	5641.48	0.0288
$h = 3$	88.18	<u>1.49</u>	1492.15	0.3818	71.36	1.73	<u>2926.48</u>	<u>0.1153</u>	64.59	<u>2.78</u>	<u>3334.70</u>	0.0427
$h = 6$	<u>91.88</u>	1.52	<u>1444.21</u>	<u>0.3990</u>	<u>77.12</u>	1.80	3175.39	0.0942	<u>57.43</u>	2.91	3996.73	0.0411
$h = 9$	92.88	1.52	1403.88	0.4025	75.40	1.45	2634.03	0.1418	53.24	2.79	1228.72	<u>0.0426</u>

Table 3. Effect of varying historical context length h on the behavior of our approach. ↑ indicates higher value is better for the metric, ↓ indicates lower value is better for the considered metric. Bold indicates the best performance of the metric while underline indicates second-best performance. Bold and underline is best performance for the primary evaluation metric LES.

manipulation choices due to incomplete information. This effect compounds with scene complexity, as larger floorplans require disproportionately more exploration to reveal critical bottlenecks. Hence, our constraint-based planner emerges as the most effective strategy for lifelong interactive navigation. We provide the implementation details for our baselines in Appendix D, and additional performance analyses in Appendix E.

4.3. Analyses

a. Effect of Manipulation Cost: To examine the behavior of our planner as the cost of manipulating objects e increases, we systematically vary the per-object manipulation cost $e \in [1, 5, 10, 15, 20]$ and measure SR, PoC, and total distance traversed by the robot (PL) across the test set (Tab. 2). We report an additional metric of Interaction Encounters (IE) that describes the percentage of obstacles the agent chose to move during the episode. As the value of e increases, IE decreases sharply across all settings, approximately $4\times$ between $e = 1$ and $e = 20$, demonstrating that the agent actively avoids unnecessary manipulation when it is costly to do so. Correspondingly, PoC rises, indicating that the planner tolerates higher clutter levels instead of restoring full connectivity at excessive expense. Despite this trade-off, SR remains largely stable, showing that the LLM-driven reasoning identifies and removes only critical obstacles essential for task completion. Path length (PL) also either remains bounded or slightly decreases, suggesting that when manipulation is de-incentivized, the agent effectively compensates by discovering alternate routes rather than interacting with high-cost obstacles. Overall, our re-

sults confirm that our constraint-based planner internalizes manipulation cost and dynamically strategizes by favoring selective, high-impact interactions over exhaustive environment cleanup, without significant degradation in SR.

b. History Length: We analyze how the amount of prior context h affects performance using LES as the primary metric (Tab. 3). In 1 – 3 rooms, LES increases monotonically with h (from 0.363 at $h = 1$ to 0.403 at $h = 9$), reflecting slightly higher SR and markedly lower TS as the planner reuses past decisions and avoids redundant exploration/manipulation. In 4 – 6 rooms, LES improves substantially with longer histories (peaking at 0.142 for $h = 9$). Although SR fluctuates, both TS and PoC benefit from better global consistency – longer context helps the LLM recall earlier constraints and target fewer, more central obstacles. In 7 – 10 rooms, $h = 3$ and $h = 9$ yield the top LES values and are essentially tied; the gain at $h = 9$ is contributed by a dramatic reduction in TS (while maintaining comparable SR and PoC), indicating that extended context accelerates progress once the agent has accumulated a rich constraint history. Overall, longer histories improve or match the best LES across all floorplans, as additional context sharpens constraint reasoning: the planner avoids revisiting explored frontiers, concentrates interactions on high-impact bottlenecks, and reduces detours—thereby balancing success, execution time, and long-term environment optimality.

c. Effect of Language Model Choice: We further evaluate the impact of different large language models within our framework in Tab. 4. Across all environment complexities, Gemini achieves the highest LES, reflecting an

LLM Name	1 – 3 rooms				4 – 6 rooms				7 – 10 rooms			
	SR↑	PoC↓	TS↓	LES↑	SR↑	PoC↓	TS↓	LES↑	SR↑	PoC↓	TS↓	LES↑
Gemini	<u>87.12</u>	1.79	2094.79	0.2179	84.09	1.67	<u>3545.79</u>	0.0946	71.06	2.73	4768.48	0.0409
GPT-5	92.27	1.44	<u>1732.55</u>	0.3771	<u>59.05</u>	<u>1.70</u>	4037.52	<u>0.0849</u>	<u>49.39</u>	<u>2.87</u>	<u>4107.61</u>	<u>0.0350</u>
Deepseek	76.21	<u>1.63</u>	1549.21	<u>0.3243</u>	51.52	1.82	2506.70	0.0767	38.03	2.94	3305.52	0.0289

Table 4. Performance of different large language models in our framework. ↑ indicates higher value is better for the metric, ↓ indicates lower value is better for the considered metric. Bold indicates the best performance of the metric, while underline indicates the second-best performance. Bold and underline is best performance for the primary evaluation metric LES.

Obstacle Density	1 – 3 rooms				4 – 6 rooms				7 – 10 rooms			
	SR↑	PoC↓	IE	TS↓	SR↑	PoC↓	IE	TS↓	SR↑	PoC↓	IE	TS↓
$d = 0.5$	<u>86.52</u>	1.31	39.24	1678.06	<u>80.91</u>	1.26	47.79	3351.85	65.00	2.50	47.39	<u>4748.91</u>
$d = 1.0$	88.94	<u>1.48</u>	39.41	1339.36	81.67	<u>1.81</u>	39.79	<u>3211.20</u>	<u>62.27</u>	<u>2.79</u>	32.70	4497.80
$d = 2.0$	81.88	3.19	16.06	<u>1592.34</u>	55.15	3.67	27.39	3135.45	48.79	4.55	23.21	4773.21

Table 5. Performance of our approach as the obstacle density varies across floorplans. ↑ indicates higher value is better for the metric, ↓ indicates lower value is better for the considered metric. Bold indicates the best performance of the metric while underline indicates second-best performance.

effective balance between success rate, environment optimality, and execution efficiency. GPT-5 performs competitively in smaller scenes but deteriorates as environment complexity increases, primarily due to its tendency to over-prioritize local obstacle relations while under-utilizing global connectivity cues in the serialized scene graph. DeepSeek (deepseek-reasoner) exhibits the weakest performance, frequently misinterpreting structured environment serializations and producing sub-optimal manipulation choices. These results highlight that model behavior, rather than raw language capability, strongly influences embodied task performance as models with compact, grounded reasoning abilities better exploit our formulation’s structural inductive biases.

d. Obstacle Density: We further assessed robustness as the obstacle density d increases from 0.5 (sparse) to 2.0 (dense), keeping task configurations fixed (Tab. 5). Overall performance declines with higher d , as reduced free space and frequent occlusions hinder long-horizon planning. In smaller layouts (1 – 3 rooms), SR drops moderately (86.5 to 81.9%), while PoC more than doubles (1.31 to 3.19), indicating diminished environment optimality. TS shows non-monotonic behavior as dense clutter sometimes shortens exploration but also causes premature failures. This trend intensifies in larger environments, where SR degrades sharply and PoC rises 2× to 3×, reflecting that, while the agent must detour or manipulate more often, it struggles to restore global connectivity. The decline in interaction encounters (IE) (from > 40% to < 30%) suggests increased conservative approach: as clutter grows, the agent avoids manipulations with low expected payoff. Together, these results highlight that higher obstacle density compounds per-

ception and reasoning difficulty, limiting the agent’s ability to maintain long-term environmental optimality.

4.4. Hardware Experiments

We validate sim-to-real transfer by deploying our framework on a Boston Dynamics Spot equipped with the Spot Arm manipulator as shown in Fig. 1. Our perception relies exclusively on the front fisheye cameras; the Spot Arm wrist camera is used only during manipulation for grasp acquisition and placement verification. The onboard state estimator provides metric localization, while stereo depth and category-level segmentations populate and update the structured scene graph in real time. Experiments are conducted in an indoor environment of a three-room setting with total navigable area of $\approx 50.0 \text{ m}^3$. We evaluate the similar tasks as in simulation, restricted to items within Spot’s gripper envelope. During operation, the scene graph is incrementally updated from fisheye RGB-D observations, enabling the planner to interleave exploration with targeted rearrangement when local bottlenecks are detected. This setup enforces the core assumptions of our setting - lifelong, partially observed, cluttered environments - while requiring no task-specific fine-tuning or hardware-specific prompts. Qualitatively, we observe that the system exhibits the same behavior as in simulation: selective removal of highly central obstacles, preference for short detours when beneficial, and robust execution of retrieve-and-place objectives under real sensing and actuation noise. We provide the implementation details of our approach on hardware in Appendix H.

5. Conclusion

Our approach redefines the role of large language models in embodied decision-making. Specifically, we recast the role of LLMs as constraint reasoners rather than sequence generators. Our method leverages structured scene graphs and cost–benefit abstractions to choose which environmental constraints to resolve, such as which obstacles to relocate where, or which regions to explore, based on their long-term impact on performance. Through extensive experiments, we showcase that our formulation enables zero-shot, long-horizon planning in unknown environments, achieving competitive task success with substantially fewer manipulations and lower cumulative cost compared to fully informed baselines. Finally, we validate the feasibility of our method on a Boston Dynamics Spot robot equipped with a depth camera and manipulator arm, demonstrating effective active perception and environment restructuring.

References

- [1] Amir Bar, Gaoyue Zhou, Danny Tran, Trevor Darrell, and Yann LeCun. Navigation world models. *2025 IEEE/CVF Conference on Computer Vision and Pattern Recognition (CVPR)*, pages 15791–15801, 2024. 1, 2
- [2] Thomas Chadzelek, Jens Eckstein, and Elmar Schömer. Heuristic motion planning with movable obstacles. In *Canadian Conference on Computational Geometry*, 1996. 3
- [3] Pang C. Chen and Yong Koo Hwang. Practical path planning among movable obstacles. *Proceedings. 1991 IEEE International Conference on Robotics and Automation*, pages 444–449 vol.1, 1991. 3
- [4] Matt Deitke, Eli VanderBilt, Alvaro Herrasti, Luca Weihs, Jordi Salvador, Kiana Ehsani, Winson Han, Eric Kolve, Ali Farhadi, Aniruddha Kembhavi, and Roozbeh Mottaghi. Proctor: Large-scale embodied ai using procedural generation. *ArXiv*, abs/2206.06994, 2022. 2
- [5] Dieter Fox, Wolfram Burgard, and Sebastian Thrun. The dynamic window approach to collision avoidance. *IEEE Robotics Autom. Mag.*, 4:23–33, 1997. 2
- [6] Samir Yitzhak Gadre, Mitchell Wortsman, Gabriel Ilharco, Ludwig Schmidt, and Shuran Song. Cows on pasture: Baselines and benchmarks for language-driven zero-shot object navigation. *2023 IEEE/CVF Conference on Computer Vision and Pattern Recognition (CVPR)*, pages 23171–23181, 2022. 3
- [7] Saurabh Gupta, Varun Tolani, James Davidson, Sergey Levine, Rahul Sukthankar, and Jitendra Malik. Cognitive mapping and planning for visual navigation. *International Journal of Computer Vision*, 128:1311 – 1330, 2017. 2
- [8] Botao He, Guofei Chen, Wenshan Wang, Ji Zhang, Cornelia Fermüller, and Yiannis Aloimonos. Interactivefar: interactive, fast and adaptable routing for navigation among movable obstacles in complex unknown environments. *2024 IEEE/RSJ International Conference on Intelligent Robots and Systems (IROS)*, pages 5402–5409, 2024. 3
- [9] Eric Kolve, Roozbeh Mottaghi, Winson Han, Eli VanderBilt, Luca Weihs, Alvaro Herrasti, Matt Deitke, Kiana Ehsani, Daniel Gordon, Yuke Zhu, Aniruddha Kembhavi, Abhinav Kumar Gupta, and Ali Farhadi. Ai2-thor: An interactive 3d environment for visual ai. *ArXiv*, abs/1712.05474, 2017. 1, 2
- [10] Obin Kwon, Nuri Kim, Yunho Choi, Hwiyeon Yoo, Jeongho Park, and Songhwai Oh. Visual graph memory with unsupervised representation for visual navigation. *2021 IEEE/CVF International Conference on Computer Vision (ICCV)*, pages 15870–15879, 2021. 2
- [11] Martin Levihn, Jonathan Scholz, and Mike Stilman. Hierarchical decision theoretic planning for navigation among movable obstacles. In *Workshop on the Algorithmic Foundations of Robotics*, 2012. 3
- [12] Hongxin Li, Zeyu Wang, Xu Yang, Yu-Ren Yang, Shuqi Mei, and Zhaoxiang Zhang. Memonav: Working memory model for visual navigation. *2024 IEEE/CVF Conference on Computer Vision and Pattern Recognition (CVPR)*, pages 17913–17922, 2024. 2
- [13] Maxim Likhachev and Dave Ferguson. Planning long dynamically feasible maneuvers for autonomous vehicles. *The International Journal of Robotics Research*, 28:933 – 945, 2008. 2
- [14] Pierre Marza, Laëtitia Maignon, Olivier Simonin, and Christian Wolf. Multi-object navigation with dynamically learned neural implicit representations. *2023 IEEE/CVF International Conference on Computer Vision (ICCV)*, pages 10970–10981, 2022. 3
- [15] Matias Mattamala, Jonas Frey, Piotr Libera, Nived Chebrolu, Georg Martius, Cesar Cadena, Marco Hutter, and Maurice F. Fallon. Wild visual navigation: fast traversability learning via pre-trained models and online self-supervision. *Autonomous Robots*, 49, 2024. 1
- [16] Arsalan Mousavian, Alexander Toshev, Marek Fiser, Jana Kosecka, and James Davidson. Visual representations for semantic target driven navigation. *2019 International Conference on Robotics and Automation (ICRA)*, pages 8846–8852, 2018. 2
- [17] Dennis Nieuwenhuisen, A.F. van der Stappen, and Mark H. Overmars. An effective framework for path planning amidst movable obstacles. In *Workshop on the Algorithmic Foundations of Robotics*, 2006. 3
- [18] Kei Okada, Atsushi Haneda, Hiroyuki Nakai, Masayuki Inaba, and Hirochika Inoue. Environment manipulation planner for humanoid robots using task graph that generates action sequence. *2004 IEEE/RSJ International Conference on Intelligent Robots and Systems (IROS) (IEEE Cat. No.04CH37566)*, 2:1174–1179 vol.2, 2004. 3
- [19] Manolis Savva, Abhishek Kadian, Oleksandr Maksymets, Yili Zhao, Erik Wijmans, Bhavana Jain, Julian Straub, Jia Liu, Vladlen Koltun, Jitendra Malik, Devi Parikh, and Dhruv Batra. Habitat: A platform for embodied ai research. *2019 IEEE/CVF International Conference on Computer Vision (ICCV)*, pages 9338–9346, 2019. 2
- [20] Philipp Schoch, Fan Yang, Yuntao Ma, Stefan Leutenegger, Marco Hutter, and Quentin Leboutet. In-sight: Interactive navigation through sight. *2024 IEEE/RSJ International*

- Conference on Intelligent Robots and Systems (IROS)*, pages 7794–7800, 2024. 3
- [21] Kunal Pratap Singh, Jordi Salvador, Luca Weihs, and Aniruddha Kembhavi. Scene graph contrastive learning for embodied navigation. *2023 IEEE/CVF International Conference on Computer Vision (ICCV)*, pages 10850–10860, 2023. 2
- [22] Xinshuai Song, Weixing Chen, Yang Liu, Weikai Chen, Guanbin Li, and Liang Lin. Towards long-horizon vision-language navigation: Platform, benchmark and method. *2025 IEEE/CVF Conference on Computer Vision and Pattern Recognition (CVPR)*, pages 12078–12088, 2024. 1
- [23] Mike Stilman and James Kuffner. Planning among movable obstacles with artificial constraints. *The International Journal of Robotics Research*, 27(11-12):1295–1307, 2008. 3
- [24] Mike Stilman and James J. Kuffner. Navigation among movable obstacles: real-time reasoning in complex environments. *4th IEEE/RAS International Conference on Humanoid Robots, 2004.*, 1:322–341 Vol. 1, 2004. 3
- [25] Xinyu Sun, Peihao Chen, Jugang Fan, Thomas H. Li, Jian Chen, and Mingkui Tan. Fgprompt: Fine-grained goal prompting for image-goal navigation. *ArXiv*, abs/2310.07473, 2023. 3
- [26] Andrew Szot, Alexander Clegg, Eric Undersander, Erik Wijmans, Yili Zhao, John Turner, Noah Maestre, Mustafa Mukadam, Devendra Singh Chaplot, Oleksandr Maksymets, Aaron Gokaslan, Vladimír Vondruvs., Sameer Dharur, Franziska Meier, Wojciech Galuba, Angel X. Chang, Zsolt Kira, Vladlen Koltun, Jitendra Malik, Manolis Savva, and Dhruv Batra. Habitat 2.0: Training home assistants to rearrange their habitat. *ArXiv*, abs/2106.14405, 2021. 2
- [27] Shagun Uppal, Ananye Agarwal, Haoyu Xiong, Kenneth Shaw, and Deepak Pathak. Spin: Simultaneous perception, interaction and navigation. *2024 IEEE/CVF Conference on Computer Vision and Pattern Recognition (CVPR)*, pages 18133–18142, 2024. 3
- [28] Hanqing Wang, Wenguan Wang, Wei Liang, Steven CH Hoi, Jianbing Shen, and Luc Van Gool. Active perception for visual-language navigation. *International Journal of Computer Vision*, 131(3):607–625, 2023. 2
- [29] Hongchen Wang, Peiqi Liu, Wenzhe Cai, Mingdong Wu, Zhengyu Qian, and Hao Dong. Mo-ddn: A coarse-to-fine attribute-based exploration agent for multi-object demand-driven navigation. *ArXiv*, abs/2410.03488, 2024. 3
- [30] Xiaohan Wang, Yuehu Liu, Xinhang Song, Beibei Wang, and Shuqiang Jiang. Camp: Causal multi-policy planning for interactive navigation in multi-room scenes. In *Neural Information Processing Systems*, 2023. 2, 3, 5
- [31] Xiaohan Wang, Yuehu Liu, Xinhang Song, Yuyi Liu, Sixian Zhang, and Shuqiang Jiang. An interactive navigation method with effect-oriented affordance. *2024 IEEE/CVF Conference on Computer Vision and Pattern Recognition (CVPR)*, pages 16446–16456, 2024. 3
- [32] Gordon T. Wilfong. Motion planning in the presence of movable obstacles. *Annals of Mathematics and Artificial Intelligence*, 3:131–150, 1988. 3
- [33] F. Xia, Amir Zamir, Zhi-Yang He, Alexander Sax, Jitendra Malik, and Silvio Savarese. Gibson env: Real-world perception for embodied agents. *2018 IEEE/CVF Conference on Computer Vision and Pattern Recognition*, pages 9068–9079, 2018. 2, 3
- [34] Xinyao Yu, Sixian Zhang, Xinhang Song, Xiaorong Qin, and Shuqiang Jiang. Trajectory diffusion for objectgoal navigation. *Advances in Neural Information Processing Systems* 37, 2024. 3
- [35] Kuo-Hao Zeng, Luca Weihs, Ali Farhadi, and Roozbeh Mottaghi. Pushing it out of the way: Interactive visual navigation. *2021 IEEE/CVF Conference on Computer Vision and Pattern Recognition (CVPR)*, pages 9863–9872, 2021. 2, 3, 6
- [36] Yiming Zeng, Hao Ren, Shuhang Wang, Junlong Huang, and Hui Cheng. Navidiffusor: Cost-guided diffusion model for visual navigation. *2025 IEEE International Conference on Robotics and Automation (ICRA)*, pages 11994–12001, 2025. 1, 2
- [37] Albert Zhai and Shenlong Wang. Peanut: Predicting and navigating to unseen targets. *2023 IEEE/CVF International Conference on Computer Vision (ICCV)*, pages 10892–10901, 2022.
- [38] Sixian Zhang, Xinhang Song, Yubing Bai, Weijie Li, Yakui Chu, and Shuqiang Jiang. Hierarchical object-to-zone graph for object navigation. *2021 IEEE/CVF International Conference on Computer Vision (ICCV)*, pages 15110–15120, 2021. 2
- [39] Sixian Zhang, Xinyao Yu, Xinhang Song, Xiaohan Wang, and Shuqiang Jiang. Imagine before go: Self-supervised generative map for object goal navigation. *2024 IEEE/CVF Conference on Computer Vision and Pattern Recognition (CVPR)*, pages 16414–16425, 2024. 3
- [40] Yuke Zhu, Roozbeh Mottaghi, Eric Kolve, Joseph J. Lim, Abhinav Kumar Gupta, Li Fei-Fei, and Ali Farhadi. Target-driven visual navigation in indoor scenes using deep reinforcement learning. *2017 IEEE International Conference on Robotics and Automation (ICRA)*, pages 3357–3364, 2016. 2

To Move or Not to Move: Constraint-based Planning Enables Zero-Shot Generalization for Interactive Navigation

Supplementary Material

A. Dataset

We construct a new dataset of cluttered indoor floors by instantiating ProcTHOR-10k simulator with procedurally generated clutter. As training set for learning baselines, we generate 10k episodes with 20 tasks each, following the Lifelong Interactive Navigation setup described in Sec. 1. Our test set consists of 100 environments equally distributed among the number of rooms 1 – 10.

To generate realistic clutter in the environment, we occlude a percentage of traversable nodes (based on floorplan area) in the grid graph $G = (N, E)$ of the unoccluded environment, where the probability of a node $n \in N$ being selected for occlusion is proportional to its betweenness centrality $bc(n)$. This biases obstacle placement toward structurally critical regions such as hallways, bottlenecks, and intersections, without deterministically blocking all high-centrality nodes. Fig. 3 shows an instance of the process of dataset generation. Fig. 8 shows examples of the generated floorplans.

B. Price of Clutter

In lifelong interactive navigation, an agent’s actions modify the physical structure of its environment, thereby influencing its future navigability. In single-goal episodes, where each episode involves completing only one task, the placement of a moved obstacle has no long-term consequence on performance. Hence, such settings offer little incentive for the agent to reason about ‘where’ to relocate an obstacle once removed. In contrast, long-horizon, multi-task episodes demand careful reasoning about object placement. An object relocated to a frequently traversed region can block critical routes, forcing repeated manipulations in later tasks. Existing interactive navigation approaches, designed for single-task settings, neither quantify such long-term environmental degradation nor explicitly optimize against it. To address this, we introduce the **Price of Clutter (PoC)** metric, which quantifies how much the environment deviates from its obstacle-free optimal configuration. Formally, we define:

$$\text{PoC} = \frac{\sum_{s,t \in N} d_{\text{obs}}(s,t)}{\sum_{s,t \in N} d_{\text{free}}(s,t)},$$

where $d_{\text{obs}}(s,t)$ denotes the shortest-path length between nodes s and t in the cluttered environment, and $d_{\text{free}}(s,t)$ is the corresponding path length in the obstacle-free environment.

Calculation: We consider two versions of the same environment \mathcal{E} : (i) a fully traversable configuration $\mathcal{E}_{\text{free}}$ with navigable graph $G_{\text{free}} = (N, E)$, and (ii) a partially occluded configuration $\mathcal{E}_{\text{curr}}$, where obstacles block certain regions, yielding a reduced graph $G_{\text{curr}} = (N', E')$. Nodes present in G_{free} may be occluded and therefore absent in G_{curr} . If either the source s or target t of a shortest-path pair in G_{free} becomes occluded, that pair is excluded from the computation since it is no longer traversable. Such occlusions indirectly increase PoC: when key nodes are removed, surviving paths between other pairs must detour around blocked regions, increasing total path lengths. For paths that originate or terminate at one of the nodes available in G_{free} but occluded in G_{curr} , the path is not traversable, and hence the length is infinite. To keep the metric finite and comparable across scales, we replace infinite distances with a capped maximum equal to $10 \times$ the maximum finite shortest-path length observed among surviving nodes. This prevents divergence in heavily occluded scenes while still penalizing disconnections proportionally to environment size.

Interpretation: A lower PoC indicates a more globally navigable and optimally structured environment, while a higher PoC means reduced accessibility and suboptimal long-term behaviour due to clutter. In our experiments, PoC serves as an indicator of how effectively the agent’s actions improve long-term environment efficiency, capturing effects that standard task success or path-length metrics fail to account for.

C. Long-term Efficiency Score

In lifelong interactive navigation, the agent must execute a sequence of navigation-manipulation tasks within the same evolving environment. Each object relocation persists and alters future navigability, meaning that decisions made for one task influence the difficulty, cost, and even feasibility of subsequent tasks. Existing metrics – such as Success Rate (SR), Time Steps (TS), Path Length (PL), Success weighed by Path length (SPL), Success weighed by Time Steps (STS), and Price of Clutter – capture only isolated aspects of performance. For example, SR does not reflect the cost of excessive detours or unnecessary object manipulation; TS alone cannot distinguish fast-but-myopic planners from methods that intentionally improve global structure; and PoC measures environment optimality but is insensitive to whether tasks are actually completed. Likewise, widely used embodied-AI metrics such as STS and SPL are designed for single-episode naviga-



Figure 3. Example dataset generation process. In this instance, we consider a 10 room floorplan from ProcTHOR-10k. The left image shows the ideal environment without clutter and completely free for optimal navigation throughout the environment. We then generate clutter in the free space using the between-ness centrality of nodes in G_{free} . The generated obstacle locations are indicated by red circles in the middle image. This causes the blocking of the paths within the accessible rooms, as well as eliminating access to the two rooms on bottom-right of the map, as shown in the right image.

tion with fixed environments – they couple success to execution efficiency, but cannot capture how object relocation reshapes future traversability, nor do they penalize environment configurations that degrade long-horizon performance. Consequently, STS and SPL reward agents that reach the goal quickly in the current environment configuration, even if their manipulations make subsequent tasks substantially harder. As a result, none of these metrics, taken independently, can evaluate long-horizon behavior or the quality of environment shaping. This motivates the need for a single, unified metric that integrates success, efficiency, and long-term environment optimality.

Calculation: Let SR denote the task success rate over an episode, TS the average number of time steps taken per episode, and PoC the Price of Clutter of the final modified environment. To ensure comparability across floorplans of different sizes and scales, we first normalize each quantity across all evaluated methods on a given floorplan group:

$$\widehat{\text{SR}} = \frac{\text{SR}}{\max_m \text{SR}_m}, \quad \widehat{\text{TS}} = \frac{\text{TS}}{\max_m \text{TS}_m},$$

$$\widehat{\text{PoC}} = \frac{\text{PoC}}{\max_m \text{PoC}_m},$$

where the maximum is taken over all methods m under comparison. The **Long-term Efficiency Score (LES)** is then defined as:

$$\text{LES} = \frac{\widehat{\text{SR}}}{\widehat{\text{TS}} \cdot \widehat{\text{PoC}}}.$$

A higher LES indicates a more efficient, globally aware agent that both completes tasks reliably and maintains a navigable environment across the full episode horizon.

Rationale Behind the Formulation: This formulation provides several advantages for evaluating lifelong interactive navigation.

- **(1) Multi-objective balance.** LES combines the three core aspects – high success rate, low time cost, and low PoC – without allowing any one metric to dominate. Methods cannot outperform each other by being fast and environmentally destructive, nor by excessively cleaning the environment to guarantee success.
- **(2) Global normalization.** By normalizing SR, TS, and PoC across all methods within each floorplan group, LES becomes comparable across environments of different sizes and obstacle densities. This enables accounting for larger environments with inflated TS or PoC and ensures consistent scaling.
- **(3) Globalized environmental assessment.** Because PoC itself is computed over all source-target node pairs in the free-space graph, LES incorporates the global impact of each manipulation action, rather than local, task-specific effects.
- **(4) Interpretability and stability.** Multiplicative coupling ensures that extreme degradation in any one dimension sharply reduces LES, reflecting the reality that a life-long agent must maintain all three properties simultaneously to remain effective.

Interpretation: High LES values indicate that an agent not only succeeds at short-term tasks but also maintains an environment whose global navigability remains close to the obstacle-free baseline environment, while completing tasks efficiently. Moderate LES corresponds to agents that solve tasks reliably but incur substantial detours or induce clutter configurations that degrade future navigation. Low LES values arise when the agent either fails frequently, manipulates objects unnecessarily, or creates highly suboptimal environments with elevated PoC. Because LES is normalized within each floorplan group, scores are directly comparable across methods and can be interpreted as a relative measure of long-term navigation efficiency: methods with higher LES consistently demonstrate better performance across the

concurrent objectives of success, path optimality, and environment shaping.

D. Baseline Implementation Details

This section provides an extended description of the baselines used in our experiments. To ensure a fair comparison, **all baseline methods, except Ours (unk), operate under full environment observability**: each method is provided with the complete map of obstacles and objects at the start of the episode, including the positions of all task-relevant objects, all drop zones for each obstacle, and all obstacles that block navigation. All baselines share the same embodiment and low-level actuation stack as our method: navigation follows a 0.25 m grid-based discretization available in ProcTHOR; manipulation is implemented via the standard `PickupObject` and `PutObject` primitives; and any failures at the level of gripper control, inverse kinematics, or grasp execution are handled by the low-level controller and does not terminate the episode. Thus, the baselines differ only in their high-level strategy for interacting with clutter and solving the navigation-manipulation objectives.

For clarity, we restate that the evaluation tasks are all object-to-object placement tasks (e.g., `Mug` \rightarrow `Shelf`, `Vase` \rightarrow `StudyTable`), and not navigate-to-region goals. All baselines attempt to complete the same 20-task sequence.

D.1. InterNav

Original capability: InterNav [35] (officially released as OBJPLACE) is designed for single-room interactive navigation using pushing actions on small tabletop or floor obstacles. The original action space consists of:

- forward/turn navigation actions,
- *push* actions, applied at pixel-level predicted contact points.

Action-space adaptation: Since our problem setting requires object rearrangement through pick-place actions rather than pushing, we replace the push primitive with `PickupObject` + `PutObject`. No modifications are made to the architecture.

Reward structure adaptation: We adapted the original reward structure to better suit our specific task requirements. To prevent the agent from prematurely terminating episodes while navigating dense clutter, we eliminated the step penalty. The task reward is distributed across the two distinct phases of the episode - navigation phase and manipulation phase. During navigation, when the agent moves towards the goal object and subsequently towards the target receptacle, the agent receives a positive geodesic reward identical to the original InterNav formulation. The sparse success reward (R_{success}) is split to encourage sub-goal completion: the agent receives $R_{\text{success}}/2$ upon suc-

cessfully picking up the correct object, and the remaining $R_{\text{success}}/2$ upon placing the object on the target receptacle.

Training setup: InterNav is re-trained end-to-end on our 10k train episodes of cluttered multi-room dataset. Each task instance (one object-to-receptacle command) serves as a single training episode. Training environments are sampled with obstacle density uniformly drawn from $d = 0$ to the maximum observed in our test split, ensuring a matched distribution.

Environment knowledge: InterNav receives full ground-truth environment information. It does not require exploration since objects, obstacles, and all occlusions are known at initialization.

Software implementation: Aside from the change in action primitives (push \rightarrow pick-place), we do not modify: its mapping logic, its pixel-level interaction predictor, its frontier selection, or its short-range navigation module.

Thus the baseline represents a faithful, strong instantiation of the published method, adapted only minimally to match the manipulation capabilities of our setting.

D.2. Always Detour

This baseline represents an extreme non-interactive strategy.

Interaction rule: The agent is forbidden from manipulating obstacles. If an obstacle lies on the current shortest path to the target object, the agent immediately declares failure.

Path computation: Shortest paths are computed using NETWORKX’s Dijkstra solver on the full ground-truth graph. Because all floorplan geometry and all obstacles are known, the path planner never needs to explore.

Consequences:

- Success depends purely on whether an entirely obstacle-free path exists.
- Never interacts with obstacles.
- Adversarially placed mild clutter can cause early termination.
- TS can be low (episodes often end quickly) but the low LES score reveals that this is purely due to avoiding meaningful interaction.

D.3. Always Interact

This baseline removes *every* encountered obstacle that blocks the shortest path to the current goal.

Interaction rule: Upon encountering an obstacle, the agent:

1. picks up the obstacle using `PickupObject`,
2. navigates to and places it at the nearest drop zone that does *not* block any path in the free-space graph (computed using ground-truth map),
3. recomputes the shortest path and continues.

Ground-truth reasoning: The baseline has complete access to all traversability information and all valid receptacle surfaces. Thus it can deterministically choose a placement that is globally non-blocking.

Characteristics:

- Removes all obstacles on the path, regardless of the consideration for long-term tasks.
- PoC is near-ideal because the agent aggressively removes everything on its immediate route.
- TS is high due to excessive manipulation.

D.4. Clean + Shortest Path (Clean + S/P)

This is an extreme over-manipulation baseline.

Interaction rule: Before attempting any task, the agent identifies *all* movable obstacles in the environment – whether or not they lie on the expected path – and removes them one by one.

Placement rule: Objects are placed at the nearest drop zone that preserves global traversability, identical to Always Interact’s placement criterion.

Execution: After full cleanup:

- all obstacles have been removed from free space,
- the environment is in a globally optimal state (PoC \approx 1.00),
- the agent executes all remaining tasks using shortest paths.

Characteristics:

- TS is extremely high due to large-scale cleanup.
- Over-interacts with obstacles in the environment.
- Environment optimality is maximal, but reasoning is naive.

D.5. Ours (Known Environment)

This variant isolates the reasoning component of our framework.

Access to full state: The LLM-based planner receives the complete scene graph at the start: all obstacles, all objects, all receptacles, and all traversability.

No exploration: The agent does not need to look for objects or reconstruct the map. The policy focuses solely on solving the sequence of tasks while strategically removing obstacles only when they improve long-term connectivity.

Interpretation: This is an upper bound on our method’s structural reasoning ability, free from challenges of partial observability.

D.6. Ours (Unknown Environment)

This is the full framework introduced in the main paper.

Sensing: The agent perceives the world exclusively through its front-facing cameras. Unlike all other baselines:

- it begins with no map,
- does not know obstacle positions,
- does not know object locations,

- must discover all task-relevant elements actively.

Active perception + LLM reasoning: The LLM receives the incrementally built scene graph and jointly chooses:

- where to explore next,
- which objects to move,
- where to relocate them,
- how to sequence navigation, manipulation, and exploration.

Low-level control: All navigation and manipulation actions are executed using the same primitives as in simulation, so comparison with baselines is fair.

Episode termination: The episode ends when:

- all 20 object-placement tasks are completed, or
- the global `max_steps` threshold is exceeded.

This baseline is the only one that must solve the *lifelong, partially observed, cluttered* problem as formulated in our paper.

E. Baseline Comparison (Extended Results)

In this section, we report two additional evaluations that highlight qualitative differences in how each baseline behaves over long-horizon episodes:

- the final Interaction Efficiency (IE) for each baseline across binned floorplans, and
- the Lifelong Environment Score (LES) plotted as a function of floorplan size.

These two metrics together quantify how selectively a method manipulates obstacles (IE) and how effectively its decisions maintain long-term environment optimality (LES).

E.1. LES Across Increasing Environment Sizes

To understand how each method scales with environment complexity, Fig. 4 plots the Lifelong Environment Score (LES) for all baselines across floorplans containing 1 to 10 rooms. LES jointly captures (i) task success across the episode, (ii) the long-term navigability of the environment as measured by Price of Clutter (PoC), and (iii) the executed time steps (TS). Thus, higher LES indicates methods that not only solve tasks but also preserve global structure and efficiency across the entire task sequence.

Small environments (1–3 rooms): In compact spaces, nearly all baselines exhibit moderate-to-high LES. This occurs because the penalty for suboptimal actions is inherently low: even aggressive strategies such as Always Interact or Clean+S/P can over-manipulate the scene with little long-term cost, while purely reactive strategies such as Always Detour can avoid manipulation entirely without incurring long detours. The limited spatial extent caps PoC, shortens detours, and reduces compounding errors, making the differences between methods less pronounced. Nevertheless, our method and the oracle variant (Ours-known) al-

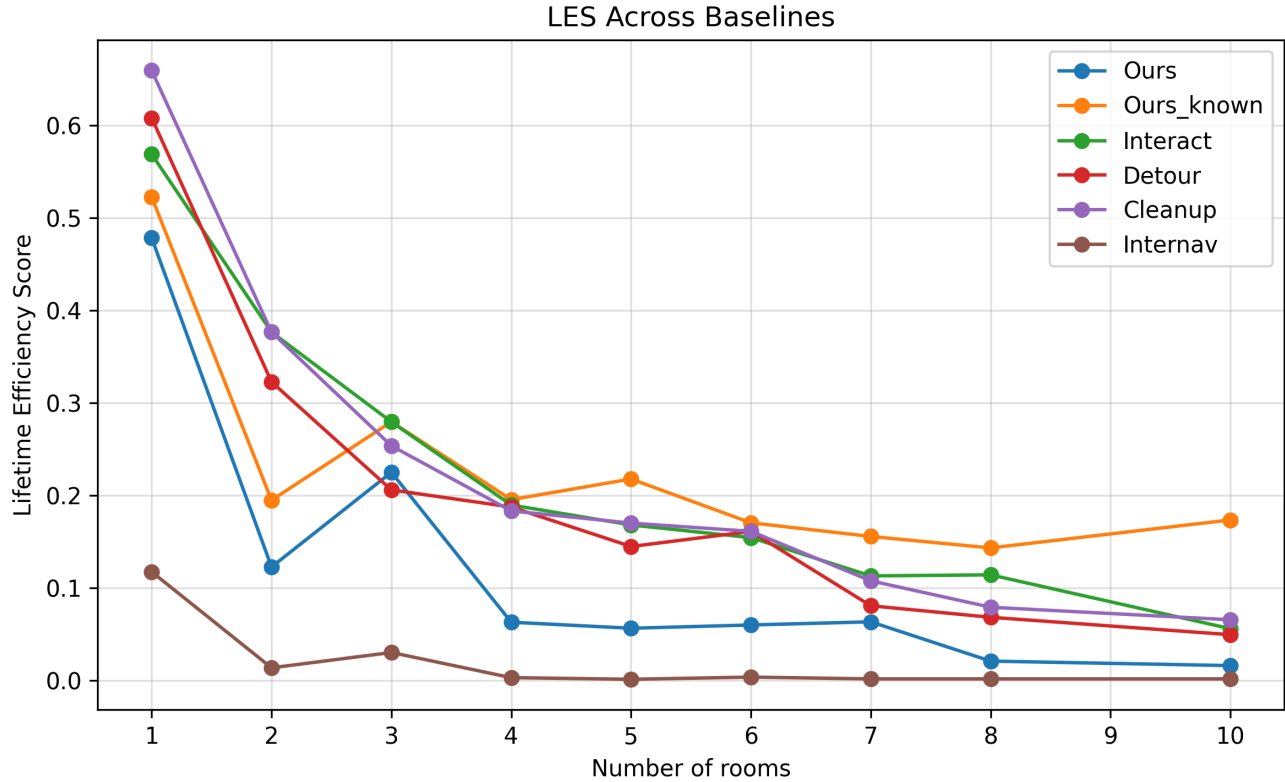


Figure 4. Lifetime Efficiency Score (LES) plot for floorplans ranging from 1 to 10 rooms. Higher is better. In small environments, nearly all baselines appear competitive because suboptimal actions – such as excessive detours (Detour) or indiscriminate manipulation (Interact, Cleanup) – incur limited long-term cost. As spatial complexity increases, these naïve policies collapse: detour-heavy strategies suffer from compounding path inefficiency, while cleanup-heavy strategies incur large manipulation overhead. InterNav fails to scale due to brittle obstacle-handling assumptions. Our method remains consistently stable across environment sizes. The widening performance gap highlights the need for selective, globally informed interaction when navigating lifelong, cluttered environments.

ready show strong LES due to more selective manipulation and shorter time-to-completion.

Medium environments (4–6 rooms): As spatial layout grows, naïve strategies begin to diverge. Always Detour and InterNav collapse quickly because never manipulating obstacles leads to increasingly long detours and frequent infeasible plans, driving LES downward. Always Interact and Clean+S/P degrade as well: although they can maintain low PoC by removing many obstacles, the large TS cost of exhaustive cleanup drags LES down sharply. In contrast, our method maintains high LES by performing targeted, high-impact rearrangements while avoiding both excessive cleanup and unbounded detours. This selective behavior retains good PoC and strong SR with considerably lower TS than cleanup-based baselines.

Large environments (7–10 rooms): In large-scale floorplans, the advantages of long-term reasoning become essential. All non-reasoning baselines experience severe LES deterioration. Detour and InterNav fail almost en-

tirely due to compounding detours, disconnected regions, and task infeasibility. Always Interact and Clean+S/P suffer from the opposite failure mode: the cost of clearing many distant or irrelevant obstacles explodes as room count increases, yielding high SR but extremely poor TS and diminished LES.

Overall, LES reveals a crucial scaling trend: In small environments, many baselines appear competitive because the cost of poor structural decisions is inherently limited. As environments grow, only methods that explicitly reason about long-term connectivity, clutter placement, and selective manipulation maintain strong performance. Our approach is the only non-oracle method whose LES curve remains significantly high and stable across all room counts, demonstrating effective lifelong planning and environment shaping.

% Interactions	1 – 3 rooms	4 – 6 rooms	7 – 10 rooms
Ours (known)	28.67	37.33	31.67
Ours (unk)	36.61	38.48	32.09
Always Interact	100.00	100.00	100.00
Always Detour	0.00	0.00	0.00
Clean + S/P	158.00	161.61	182.47

Table 6. Percentage of interactions (IE) executed by each baseline across the three floorplan bins.

E.2. Interaction Efficiency Across Floorplans

To complement the LES analysis, we examine the percentage of interactions (IE) executed by each baseline across the three floorplan bins (Table 6). IE measures how often an agent chooses to manipulate obstacles relative to the number of obstacles it encounters. Since excessive manipulation is costly in both time and long-term structural distortion, IE captures a core determinant of high LES.

A clear trend emerges: methods with extreme interaction policies achieve the lowest LES in large environments. **Always Interact** performs 100% manipulation regardless of context; this directly explains its sharp LES drop as room count increases (Fig. 4). **Clean + S/P** is extremely aggressive in obstacle manipulation – it removes all obstacles before solving any of the tasks – leading to IE values greater than 150% as it manipulates more obstacles than it ever would encounter along optimal routes. These policies appear competitive in small environments, where their heavy-handed behavior does not incur substantial penalties; however, as free-space geometry becomes more complex, such over-interaction drastically harm long-horizon efficiency, reflected in steep LES decay.

Conversely, **Always Detour** maintains 0% IE by design. While this avoids direct manipulation costs, it forces the agent into long navigation routes whenever clutter blocks high-connectivity regions. In larger floorplans, these detours accumulate geometric inefficiencies that outweigh any benefits of interaction frugality, again explaining its lowering LES values as the number of rooms increases.

Our methods – **Ours (unk)** and **Ours (known)** – have IE values in moderate range (28–38%), increasing slightly with floorplan size as more rooms imply a higher chance of encountering globally central obstacles. Unlike the over-reactive baselines, our approach interacts only when doing so meaningfully improves long-term navigability – the behavior rewarded by LES. The LES curves reflect this: while all baselines degrade as room count increases, our approach maintains significantly higher efficiency, with **Ours (known)** forming an approximate upper bound on selective, globally informed rearrangement.

Together, these results show that only planners capable of evaluating global structure – rather than reacting myopi-

cally to local blockages – achieve this balance consistently across floorplan scales.

F. Obstacle Density Experiments: Comparison with Baselines

To assess the robustness of our framework under varying clutter conditions, we evaluate all baselines across three obstacle densities: $d = 0.5$ (sparser than standard), $d = 1.0$ (default dataset density), and $d = 2.0$ (highly cluttered scenes), using identical environments and task sequences. Across all densities, we report Success Rate (SR), environment optimality (PoC), time steps (TS), and our unified long-horizon metric LES. The results are summarized in Tab. 5. In sparser environments ($d = 0.5$), all methods benefit from increased free space, but the relative ordering remains informative. Our known-map variant achieves the highest LES in the small-room regime (0.6708), and remains competitive in medium and large scenes (0.3410 and 0.2088), exceeding or matching the best non-LLM baselines except for the trivial Clean+S/P policy – which incurs no perception or reasoning cost and clears all obstacles regardless of necessity. The unknown-map variant performs moderately lower due to required exploration, but still remains comparable to the heuristic baselines, particularly outperforming Detour in dense connectivity settings where proactive interaction matters. At standard density ($d = 1.0$), the expected trend reappears: sparser-environment scores reduce, and differences across strategies become more pronounced. Our known-map policy again maintains strong LES in all room bins (0.3322, 0.1945, 0.1574), while the heuristic methods begin to degrade with scale – Always Interact loses efficiency due to unnecessary rearrangements, and Detour suffers from high PoC as path options collapse. Clean+S/P remains an upper bound but achieves this by forcing extreme over-interaction (IE \geq 150%). In highly cluttered scenes ($d = 2.0$), the compounding challenge of limited visibility, restricted free space, and high occlusion amplifies the penalties on all baselines. LES drops sharply across the board. Yet, importantly, our known-map method remains the second-best performer in medium and large environments, surpassed only by Clean+S/P – which has unfair advantage as it clears every obstacle at the start, ignoring task cost and violating real-world practicality. The unknown-map version experiences the largest decline (e.g., LES = 0.1747 to 0.0321 to 0.0152) because exploration itself becomes more expensive and clutter physically restricts reachable areas. Nevertheless, even in this extreme setting, our approach does not collapse to the levels of InterNav or Detour, indicating that our long-horizon reasoning still identifies and manipulates structurally influential obstacles rather than acting reactively. Overall, these results confirm that LES reliably captures the degradation in navigability and long-horizon efficiency as clutter increases, and that our

Obstacle Density	1 – 3 rooms				4 – 6 rooms				7 – 10 rooms			
	SR	PoC	TS	LES	SR	PoC	TS	LES	SR	PoC	TS	LES
d = 0.5												
Ours (known)	95.61	1.10	931.45	0.6708	100.00	1.11	1762.58	0.3410	94.85	1.30	2384.24	0.2088
Ours (unk)	86.52	1.31	1678.06	0.4001	80.91	1.26	3351.85	0.1302	65.00	2.50	4748.91	0.0489
Always Interact	100.00	1.07	1026.18	0.6699	100.00	1.32	2043.97	0.2702	100.00	1.35	3359.55	0.1625
Always Detour	87.88	1.37	707.06	0.6695	86.97	1.68	1240.48	0.2810	73.48	2.65	1620.52	0.1313
Clean + S/P	100.00	1.00	1107.71	0.6501	100.00	1.00	2126.58	0.3104	100.00	1.00	4320.03	0.1530
d = 1.0												
Ours (known)	94.55	1.50	1044.55	0.3322	97.73	1.25	1911.97	0.1945	100.00	1.23	2435.48	0.1574
Ours (unk)	88.94	1.48	1339.36	0.2753	81.67	1.81	3211.20	0.0598	62.27	2.79	4497.80	0.0344
Always Interact	100.00	1.14	1108.88	0.4082	100.0	1.13	2416.67	0.1707	100.00	1.36	3974.88	0.0943
Always Detour	90.45	1.96	665.64	0.3788	83.18	2.15	1115.27	0.1644	64.09	3.43	1381.61	0.0661
Clean + S/P	100.00	1.00	1200.48	0.4297	100.00	1.00	2622.94	0.1714	100.00	1.00	5169.58	0.0841
d = 2.0												
Ours (known)	94.55	2.56	915.76	0.2987	92.88	2.46	2014.21	0.1522	92.88	2.49	2904.09	0.0877
Ours (unk)	81.88	3.19	1592.34	0.1747	55.15	3.67	3135.45	0.0321	48.79	4.55	4773.21	0.0152
Always Interact	100.00	1.41	1314.16	0.3904	100.00	1.72	2953.97	0.1406	100.00	1.45	5135.61	0.0925
Always Detour	84.85	3.30	386.48	0.3491	41.67	4.66	541.42	0.1161	38.18	5.40	714.82	0.0686
Clean + S/P	100.00	1.00	1457.42	0.3280	100.00	1.00	3609.36	0.1666	100.00	1.00	6879.50	0.0810

Table 7. Comparison of our approach with baselines across different floorplans under varying obstacle densities.

method remains competitive and structurally grounded even under severe occlusions, outperforming practical heuristic baselines and trailing only the trivial exhaustive-cleanup policy.

G. System Behaviour with Episode Horizon

To assess the robustness of our method under varying long-horizon episodes, we evaluate all baselines across episodes containing 10, 15, and 20 sequential object-placement tasks, keeping environments and goal configurations fixed (Tab. 8). Because each additional task compounds both navigation and manipulation consequences, this setting indicate whether a method can maintain accumulated environment optimality rather than simply succeed at isolated goals. Across horizons, our approach – both with known maps and unknown maps – remains consistently competitive under the Lifetime Efficiency Score (LES). In shorter episodes ($g = 10$), the known-map variant achieves the highest LES in all floorplan bins, reflecting its ability to strategically modify the environment early and leverage those improvements repeatedly. The unknown-map variant, despite requiring active exploration, still outperforms detour-based and cleanup-based baselines, indicating that its longer-term reasoning compensates for the overhead of discovery. As the horizon increases to $g = 15$, LES values decline for all methods, but the drop for our approach is significantly smaller than for non-reasoning baselines. Always-Detour and Always-Interact suffer from horizon amplification: detouring repeatedly accumulates suboptimal transit cost, while interacting excessively compounds manipula-

tion penalties - both effects lowering LES. Clean+S/P remains strong for small scenes but deteriorates with scale, since aggressive early cleanup no longer amortizes over many tasks in larger environments. In contrast, our method adapts its interaction strategy to horizon length, removing only high-centrality obstacles whose impact propagates across many tasks, keeping PoC low without incurring excessive TS. In the most demanding setting ($g = 20$), our method with known maps continues to rank among the top-two performers across all floorplan scales, and remains within a small margin of the best LES in large (7 – 10 room) scenes. Meanwhile, other baselines exhibit widening failure modes: Always-Interact and Clean+S/P incur escalating TS due to unnecessary manipulation, while Detour becomes progressively worse as repeated long-path navigation dominates total cost. Even the unknown-map variant – despite substantial exploration overhead – remains competitive under LES, demonstrating stability absent in all heuristic baselines. Overall, these results highlight that LES sharply differentiates myopic strategies from genuinely long-term policies, revealing that methods lacking global reasoning degrade rapidly as episode horizons lengthen. In contrast, our approach, through explicit reasoning about environment structure, maintains efficient lifelong performance.

H. Hardware Deployment

We deploy our method on a Boston Dynamics Spot robot equipped with the Spot Arm, demonstrating that our system transfers from simulation to a real mobile manipulator. Below, we describe the full hardware pipeline used in our

Episode Horizon	1 – 3 rooms				4 – 6 rooms				7 – 10 rooms			
	SR	PoC	TS	LES	SR	PoC	TS	LES	SR	PoC	TS	LES
g = 10												
Ours (known)	98.79	1.29	578.88	0.9472	100.00	1.28	1040.42	0.5038	90.61	1.54	1594.36	0.2591
Ours (unk)	93.33	1.85	675.52	0.6611	72.42	2.12	2099.79	0.1155	65.45	3.00	2270.42	0.0837
Always Interact	100.00	1.19	681.79	0.8951	100.00	1.37	1521.58	0.3451	100.00	1.16	2565.52	0.2248
Always Detour	87.88	2.34	364.48	0.8229	86.36	2.10	613.52	0.4516	66.06	3.23	758.76	0.1963
Clean + S/P	100.00	1.00	835.72	0.8411	100.00	1.00	1909.91	0.3352	100.00	1.00	3865.10	0.1443
g = 15												
Ours (known)	100.00	1.22	814.48	0.7453	97.78	1.20	1403.76	0.3877	94.14	1.57	2356.94	0.1910
Ours (unk)	94.14	1.53	857.79	0.5450	79.41	1.46	2049.79	0.1885	64.85	2.88	2843.94	0.0632
Always Interact	100.00	1.15	905.39	0.7044	100.00	1.34	1983.30	0.2670	100.00	1.15	3321.25	0.1771
Always Detour	84.04	2.19	505.30	0.5864	84.44	2.09	878.97	0.3085	66.26	3.21	1094.18	0.1373
Clean + S/P	100.00	1.00	1075.30	0.5282	100.00	1.00	2383.58	0.2708	100.00	1.00	4693.99	0.1324
g = 20												
Ours (known)	94.55	1.50	1044.55	0.3322	97.73	1.25	1911.97	0.1945	100.00	1.23	2435.48	0.1574
Ours (unk)	88.94	1.48	1339.36	0.2753	81.67	1.81	3211.20	0.0598	62.27	2.79	4497.80	0.0344
Always Interact	100.00	1.14	1108.88	0.4082	100.00	1.13	2416.67	0.1707	100.00	1.36	3974.88	0.0943
Always Detour	90.45	1.96	665.64	0.3788	83.18	2.15	1115.27	0.1644	64.09	3.43	1381.61	0.0661
Clean + S/P	100.00	1.00	1200.48	0.4297	100.00	1.00	2622.94	0.1714	100.00	1.00	5169.58	0.0841

Table 8. Comparison of our approach with baselines across different floorplans across varying task horizons.

experiments.

H.1. Perception and Object Recognition

Spot is equipped with five front-facing fisheye cameras and a wrist-mounted depth camera on the end-effector. To remain faithful to our simulation assumptions, we restrict active perception during navigation to only the front fisheye RGB-D streams; the wrist camera is used exclusively during grasping and placement to ensure reliable manipulation. Object detection on fisheye images is performed in a two-stage process:

1. **Label prediction:** We run a YOLO-based detector to obtain coarse object categories that match our simulation-level abstractions (e.g., Mug, Box, Shelf, StudyTable).
2. **Mask generation:** For each detected object, we apply SAM to obtain a high-quality bounding region and mask, which is then projected into 3D using the synchronized depth image.

Detected objects are inserted into the scene graph, maintaining the same representation used in simulation.

H.2. Environment Representation and State Estimation

Since the physical lab layout is fixed and known, we pre-compute a ground-truth grid graph of traversable free space prior to the episode. This graph uses a grid resolution of 1.0 m, and is used for shortest-path planning, betweenness estimation, and PoC computation.

Spot’s pose within this map is obtained using its onboard state estimator, which fuses IMU, kinematic odometry, and visual-inertial sensing. This provides a drift-minimized, metrically consistent localization signal throughout the episode, enabling us to register detections, depth maps, and manipulated-object trajectories directly into the global coordinate frame.

During execution, the robot maintains an estimate of currently reachable nodes. For any grid node, we evaluate the local 3D occupancy by analyzing the point cloud density inside a spherical region of fixed radius. Let $S(v)$ denote the set of depth points within the sphere centered at node v . A node is marked *occupied* if $|S(v)| > \tau$ and *free* otherwise. We set the occupancy threshold to $\tau = 400$, selected empirically to balance noise suppression and spatial sensitivity.

This online occupancy classification yields a dynamically evolving traversability graph that the LLM planner queries when reasoning about shortest paths, obstacle-induced bottlenecks, and candidate regions for exploration.

H.3. Low-Level Control and Execution

All locomotion and manipulation commands are executed using the official `bosdyn` Python SDK. Our system interfaces with Spot via:

- **Navigation:** issuing waypoint-based locomotion goals generated by the mapping module,
- **Manipulation:** using the SDK’s grasp and arm-trajectory APIs for pickup and placement.

The low-level controller provides robust execution primitives such as:

- grasp acquisition with automatic force adjustment,
- hand-equipped alignment during approach,
- arm release and retreat after placement.

These behaviors abstract away most failures at the control layer, allowing the high-level LLM planner to focus on reasoning about obstacle configuration, exploration, and task sequencing.

H.4. Runtime Integration

At each control cycle, the system:

1. captures front-camera RGB-D observations,
2. runs YOLO+SAM to update scene graph entries,
3. updates the reachable grid nodes using depth-based occupancy,
4. queries the LLM for the next high-level action (navigate, pick-and-place, or explore),
5. executes the corresponding low-level command through the `bosdyn` API.

This forms a tight perception–reasoning–action loop that closely mirrors our simulator setup while operating under real sensor noise, partial observability, and actuation uncertainty.

H.5. Real Robot Experiments

We provide visualization of an episode executed on Spot robot. Fig. 5 shows the point cloud and observed free navigable space as seen by the robot.

I. Prompts

To facilitate full transparency and reproducibility of our method, we provide the exact system-level (Fig. 6) and developer-level (Fig. 7) prompts used to guide the LLM planner in our framework for constrained-based planning. Our prompts precisely encode the rules of our setting – long-horizon, sequential-tasks, partially observed interactive navigation – and expose to the model only those abstractions available to the robot at test time (e.g., scene-graph structure, obstacle costs, path characteristics, and remaining task budget). By doing so, the prompts serve as an explicit interface between high-level reasoning and low-level execution: they constrain the LLM to operate within the capabilities of the underlying planner while enabling flexible, global decision-making about exploration, obstacle relocation, and long-term environment shaping.

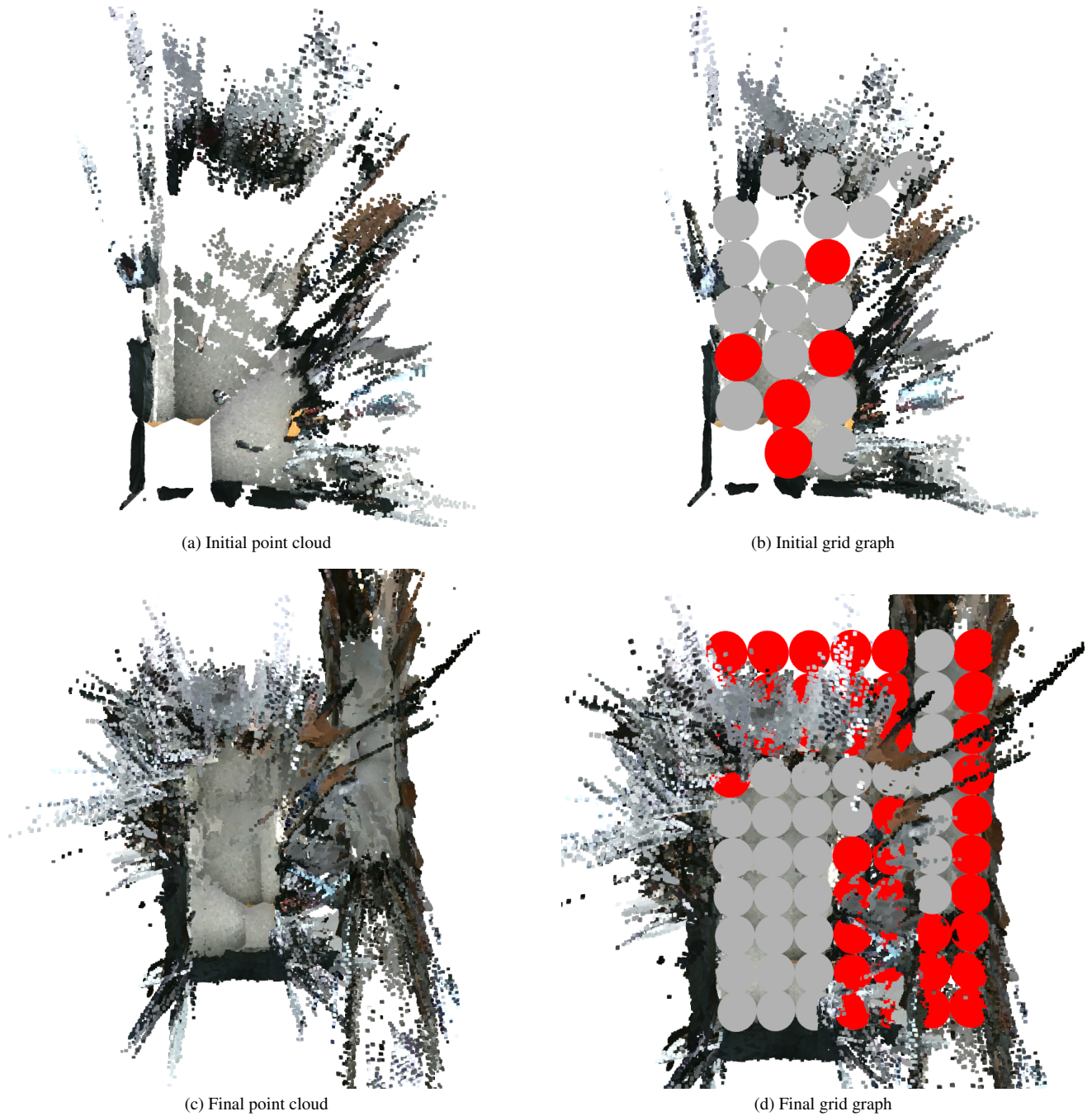


Figure 5. Point-cloud-driven environment mapping during real-world deployment. We visualize the evolution of the robot’s perception and its derived navigation graph during a real episode on the Boston Dynamics Spot. (a) The initial RGB-D observations from the front fisheye cameras produce a sparse and noisy point cloud reflecting partial scene coverage. (b) From this point cloud, the system constructs an initial navigation grid graph by projecting points onto the 2D floor plane and classifying nodes as free (gray) or occupied (red) based on local point density and presence of obstacles. (c) As the robot actively explores and executes navigation and manipulation actions, the accumulated point cloud becomes significantly more complete, revealing previously unseen regions and freed regions due to obstacle relocation. (d) The final grid graph incorporates these expanded observations, yielding a more accurate and globally connected representation of traversable space and obstacles. This perception-mapping loop provides the structured scene graph used by our LLM planner to reason about exploration, obstacle relocation, and long-horizon navigation decisions.

System Prompt

You are a robot planner. You are in an ai2thor simulator environment. You will be given multiple tasks one after another. Each task consists of a goal object type and a target object type. You have to retrieve the object that satisfies the goal object type and place it on the target object type. The environment is multi-room floorplan with multiple rooms and has many objects.

Your input is a scene description of the objects discovered so far.

Your policy -

- Explore the different rooms until you discover the objects relevant to your goal. Exploring the rooms populates the scene description.
- From the built scene description, you should first choose which goal object to move to for completing the task.
- Once you have decided the object, use the tool named "get_obj_path_data" to retrieve the characteristics of the path that leads from your location to the specified object. This path data will contain information such as the names of obstacles on the shortest path, the cost of reaching this object, etc.
- Use this path data to decide your plan. You can either "avoid" an obstacle on the path, or you can "interact" with the obstacle on the path. If you decide to "avoid" an obstacle, that means you want to take a path that is longer than the shortest path obstructed by this object, but unobstructed by this object. If you choose to "interact" with an obstacle, that means you want to pick-up that obstacle and place it somewhere else so that your path is free for traversal. Use the tool named "get_obstacle_data" to find out which receptacles are available for each of the objects so that you can decide which ones to "avoid" and which ones to "interact" with.
- Once you have decided the final plan of which obstacles to avoid/interact, and where each interact object goes, call the tool "execute_plan" to execute the plan in the environment. You should always output your final plan since no re-assessment opportunities will be provided.

There are 6 types of entries in the scene description provided to you -

"goal" describes your current task.

"progress" describes how many tasks out of total tasks you have completed

"reward_gained" describes the reward you have gained till now.

"total_cost" describes the cost of taking the past actions.

"room_visit_counter" describes the number of timesteps you have spent in each room.

"robot" describes your current state in the environment and your possible next actions.

The "robot" section has following fields -

"inventory" - Contains the object ID and type of the object you are currently holding.

"currently_in_room" - Describes the ID of the room you are currently in.

"current_room_type" - The type of room you are currently in.

"valid_navigation_actions" - Describes the navigation actions that you can attempt relative to current robot position and orientation. In case you cannot take an action, describes the reason why that action is invalid.

"position" - Dict data type. Describes the coordinates of your centroid.

"looking_at" - String data type. Describes the direction you are looking at.

The "valid_navigation_actions" has following field for each object you can navigate to -

"shortest_path_exists" - A boolean describing whether an obstacle free shortest path to that object exists from your current position.

"path_blockers" - List of names of the obstacles that block the shortest path leading to the object from your current position.

"shortest_path_cost" - The cost of traversing this shortest path.

"cost_to_free_shortest_path" - In case the shortest path to the object does not exist due to being obstructed by an object, describes the cost to reach that object and free up the shortest path.

"percentage_paths_freed_upon_removal_of_this_object" - Describes the betweenness centrality of the node occupied by the blocker object of the shortest path.

"detour_path_exists" - Describes whether it is possible to detour around the object blocking shortest path to reach the object via a longer path.

"detour_path_cost" - Cost to traverse the path that avoids the obstacles blocking the shortest path to this object.

Figure 6. Our system prompt for the Large Language Model in our constraint-based planning framework.

Developer Prompt

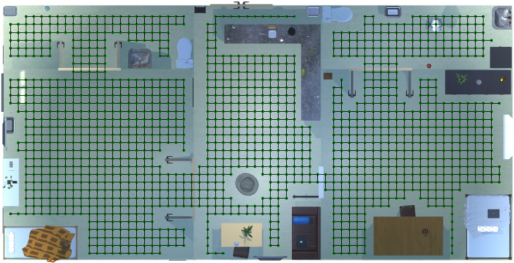
Your policy -

- You have to modify the environment for long-term navigation by removing the blocking obstacles out of the way while completing the given tasks and keeping the long-term cost low.
- Early in the episode, prefer to move the low-medium "cost_to_remove_this_object" obstacles. Near the end of the episode, focus on completing remaining tasks by detouring around obstacles. Compare the value of cost_to_remove_this_object and shortest_path_cost to figure out if you should move the object or not.
- If the scene description says that the 'times_scanned' status of a room is '0', you need to scan the room so that you can discover the path to other rooms connected to your current room.
- Scan the room multiple times (max 3 times) to make sure you discover most of the objects kept in the room.
- Make sure you can find at least one instance of goal object and target object in your scene description. If not, then you need to explore the environments by going to the room that has the highest likelihood of finding the objects you are looking for. Keep exploring until you discover them.
- Revisit different rooms multiple times for scanning (scan_room) to discover hidden objects that you could not discover the first time you visited.
- Do not trigger execute_plan until you have found a receptacle object in the scene that satisfied the given task.
- Retrieve the goal object only after you have discovered at least one instance each of goal object and target receptacle object in your scene graph.
- Do not optimize for immediate cost. Optimize for long-term cost based on remaining number of tasks.
- You do not have to move all the obstacle objects on your path. You can choose to move a subset of them that are most rewarding in terms of the number of paths they block.
- Decide whether to "interact" or "detour" for each obstacle object based on the quantities provided to you - how many tasks are left, cost of bringing the object to receptacle, the minimum cost of reaching the goal position from the receptacle, the obstacles that lie in the minimum cost path, hence pushing the cost up.
- When you clear the obstacles, some shortest paths become free which enable you to complete the future tasks efficiently.

Figure 7. Our developer prompt for the Large Language Model in our constraint-based planning framework.



(a) Occlusion in room 1 floorplan



(b) Occlusion in room 5 floorplan



(c) Occlusion in room 10 floorplan

Figure 8